NUMERICAL AEROACOUSTIC ANALYSIS OF SMALL COOLING FANS FOR ELECTRONIC DEVICES

Alexis TALBOT[1], Yves DETANDT[1],
Shogo HATANAKA[2], Kenichiro HIRAI[2], Gaku MINORIKAWA[3]

[1] *Free Field Technologies, MSC Software Belgium, Rue Emile Francqui 9*
1435 Mont Saint Guibert, Belgium

[2] *Software Cradle Co., Ltd, 3-4-5, Umeda, Kita-ku*
Osaka 530-0001, Japan

[3] *Hosei University, Department of Mechanical Engineering,*
Faculty of Science and Engineering, Tokyo, Japan

SUMMARY

The optimization of an electronic fan design can be done by means of numerical simulations taking into account aerodynamic and acoustic performances. For aerodynamics, simplified CFD analyses can be run in a relatively short time frame to evaluate the performances of new designs. For acoustics, however, the CFD analysis needs to be much more complex and accurate to resolve the acoustic part at the same time. This paper presents an approach to simulate electronic fan noise based on a hybrid (CFD + Acoustic) method relying on the Lighthill analogy. The method is applied on three configurations of an electronic fan and compared to measurement results.

INTRODUCTION

Most electronic devices require efficient cooling systems to operate correctly. Fans often take an important place in this cooling system, extracting the heat outside the casing. As these electronic components are present in quiet environments (home, office, conference rooms) and acoustic performances represent a competitive advantage for fan suppliers, the cooling systems in general and fans in particular have to be as quiet as possible.

The aerodynamic and thermal performances are predicted by means of computational fluid dynamics (CFD) simulations. To name but a few, the number of blades, the blade shape, and the rotation speed are parameters which are optimized. These parameters will also have an influence on the acoustic signature of the fan. Some dominant tonal components may be critical for instance and acoustic simulation results can be integrated in this optimization process.

In this paper, we compare the noise generated by cooling fans which have the same size, but which differ by their parameters (number of blades, blade profile…). In the first part of the paper, the computational process is presented, and the different parameters of the aeroacoustic simulation (including CFD and acoustic solver parameters and models) are presented and discussed. In the second part, the methodology is applied to 3 different configurations of an electronic fan case. For each configuration, experimental measurements are available to assess validity of the numerical results. The objective of this second part is to validate the use of simulation in this optimization process.

COMPUTATIONAL PROCESS

The computational process is decomposed in several steps as sketched in Figure 1 to estimate the aerodynamic and acoustic performances. The process assumes that the flow generates acoustic sources and that acoustics will not trigger specific turbulence structures or impact on the flow field.
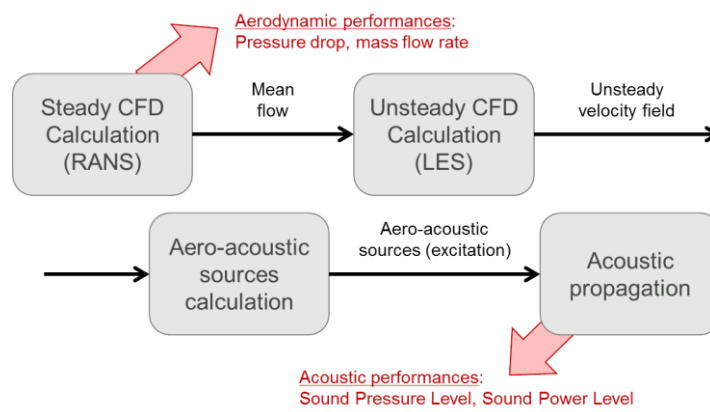

Figure 1 - Overview of numerical simulation process for aerodynamic and acoustic fan performances prediction

Steady CFD calculation

The process requires an initial fully developed flow field generated by a steady CFD calculation. Starting from this established flow field avoids long transient simulations and therefore saves resources for the second step. This step also provides useful information on performances for several operating conditions (the characteristic P-Q curve for instance).

The solution is derived by solving the Reynolds Averaged Navier-Stokes equations (RANS). The turbulence model needs to represent the effects of unsteady fluctuations on averaged flow profile:

- Turbulence Model: SST k-ω model developed by Menter [1], generally suited for separated flows,
- Boundary condition: The domain extends to the experimental chambers to represent all possible large recirculating flows around the fan. The CFD domain could be reduced by applying more advanced inflow conditions, but this is not the case for all current CFD simulations
- Pressure correction method: SIMPLE algorithm
- Accuracy of convective terms: 2nd order upwind scheme

Unsteady CFD calculation

As aeroacoustics is dealing with flow unsteadiness, the source extraction needs an unsteady flow solution in the volume enclosing the fan. Large Eddy Simulations (LES) or Detached Eddy Simulations (DES) provide accurate flow solution. To trigger turbulence more rapidly from the initial steady solution, some stochastic fluctuations (velocity and pressure) are added to the initial

solution. This requires a lower number of iterations to reach the fully developed turbulent flow where the solution will be recorded for noise source extraction.

The unsteady simulation (LES) parameters are the following:

- Turbulence model (SGS model): WALE model (Wall-Adapting Local Eddy-viscosity model). WALE model is suited to reproduce accurately the near-wall behavior [2].
- Accuracy of convective terms: Blending scheme of 1st order upwind and 2nd order central difference schemes using Gamma limiter blending method [3]. An effect of a 1st upwind scheme is introduced into the advection term to ensure the stability of calculation.
- Accuracy of time derivative term: 2nd order implicit scheme
- Pressure correction method: SIMPLEC algorithm

Aero-acoustic sources calculation

Acoustics is generated by the unsteady phenomena related to turbulence. The acoustic and fluid dynamics signals are mixed in the source region. The acoustic part, although being very small compared to the aerodynamics one is very efficient and propagates over large distances without any major dissipation. The aeroacoustic sources region corresponds to the zone where the most active turbulent eddies are located. For fan noise application, the rotor generates a series of harmonics related to the blade passages associated to rotation, but the blades wakes also include smaller turbulent structures responsible for a broadband part of the noise.

Several methods have been developed to tackle this problem, from analytical methods with fast resolution times to advanced and computationally expensive direct simulation where both fluid dynamics and acoustics perturbations are solved at the same time. In this hybrid method, the aeroacoustic sources are computed from a reliable unsteady CFD solution and then propagated in an acoustics dedicated solver. The input unsteady flow field needs to represent accurately the turbulent physics in order for the aeroacoustic sources to be accurate. This separation between the flow and acoustic parts of the problem saves the computational resources as each part method is optimized, and aligned with the physics requirements:

- Amplitude: the fluid pressure fluctuations driving the flow are much larger than the acoustic pressure fluctuations. Capturing acoustics in the flow simulation therefore requires accurate and non-dissipative schemes.
- Propagation speed: The Mach number is the ratio between the fluid velocity and the speed of sound. The maximum propagation speed has an influence on the flow simulation time step.
- Length scale: the turbulent length scales are much shorter than the acoustic wavelength, leading to a very different spatial resolution for turbulence and acoustics modeling

This split of the problem where the preliminary computed unsteady flow is processed to extract the noise sources in a second step is called the hybrid approach. It assumes that acoustics does not provide any feedback effect on the fluid dynamics. The hybrid approach has been proposed originally by Lighthill [4] but several scientists [5] propose similar techniques, differing by the equation solved or by the technique used to solve the mathematical equation.

For the present application, a Finite Element Method (FEM) solver is used to derive a frequency domain solution of the Lighthill equation (1) as detailed in [6]:

$$\frac{\partial^2 \tilde{\rho}}{\partial t^2} - \frac{\partial}{\partial x_i}\left(c_0^2 \frac{\partial \tilde{\rho}}{\partial x_i}\right) = \frac{\partial^2 \tilde{T}_{ij}}{\partial x_i \partial x_j} \qquad (1)$$

where the Lighthill equation is solved for density fluctuations $\tilde{\rho}$, providing that the Lighthill tensor $\widetilde{T_{ij}}$ is computed from the unsteady solution. The equation is solved in the frequency domain. The FEM formulation right hand side includes a volume contribution corresponding to the aeroacoustic sources present in the computational domain and a surface integral accounting for all sources present upstream and convected through a permeable boundary:

$$\omega^2 \int_V N_a \rho \, dV - \int_V \frac{\partial N_a}{\partial x_i} c_0^2 \frac{\partial \rho}{\partial x_i} dV = i\omega \oint_S N_a \rho v_i n_i dS + \int_V \frac{\partial N_a}{\partial x_i} \frac{\partial T_{ij}}{\partial x_j} dV \qquad (2)$$

where:

- ω is the angular frequency
- v_i is the ith component of the velocity
- ρ is the acoustic density fluctuation
- N_a is the finite element shape function
- $\widetilde{T_{ij}}$ is the Lighthill tensor

The acoustic domain does not include the rotating blades and the surface contribution needs to be computed on the permeable surface enclosing the rotor. As CFD schemes are mainly designed to capture the turbulent field, they are in general dissipating the acoustic signal rapidly. To capture the signal in a region where the information is still accurate, techniques have been developed in the solver to read the information in the rotating part where the blade wakes signals are accurate and reliable for acoustic propagation.

Acoustic propagation

The acoustic propagation consists in solving the Lighthill equation (1) by means of a finite elements modeling. The computational domain is discretized by a mesh. The local material and thermodynamical properties are defined to match to experimental conditions. The mesh is made with linear elements. The domain is meshed with at least 10 elements per acoustic wavelength which gives a good accuracy level (low dissipation and dispersion).

The non-reflecting far field condition is modelled by means of infinite elements for the exterior envelope of the model. The rotating part is not included in the acoustic model, the boundary integral contribution being computed on this interface to provide the noise excitation emanating from the fan wakes.

In the present paper, the main objective is to validate the method on a free field fan radiation problem. Integrating this cooling fan in electronic devices would require to use additional boundary conditions (duct ends, porous materials, heat exchanger …) which are available in the solver and been validated in the literature. The casing of the electronic device could be included in the simulation to check if the casing vibrations may affect the exterior noise level.

APPLICATION ON ELECTRONIC FAN CASE

Model description

The application case shown in Figure 2 consists of a 111 mm diameter electronic fan supported by 4 spokes in a plastic casing. The spokes are evenly distributed and the internal envelope of the casing enclosing the fan is perfectly circular.
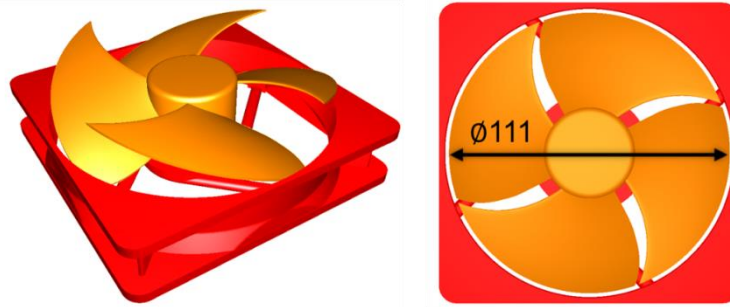
Figure 2: Baseline configuration of electronic fan

Several models have been tested experimentally varying the geometrical parameters with respect to the reference baseline configuration. These experimental tests highlight the influence of the parameters on the acoustic performances of the fan. The variations include changes on the number of blades and shape of the blades, including modification of the inlet, outlet, rake and skew angles. All tested variations are presented in Figure 3. For all tested case, the rotation speed is set to 3300 rpm.
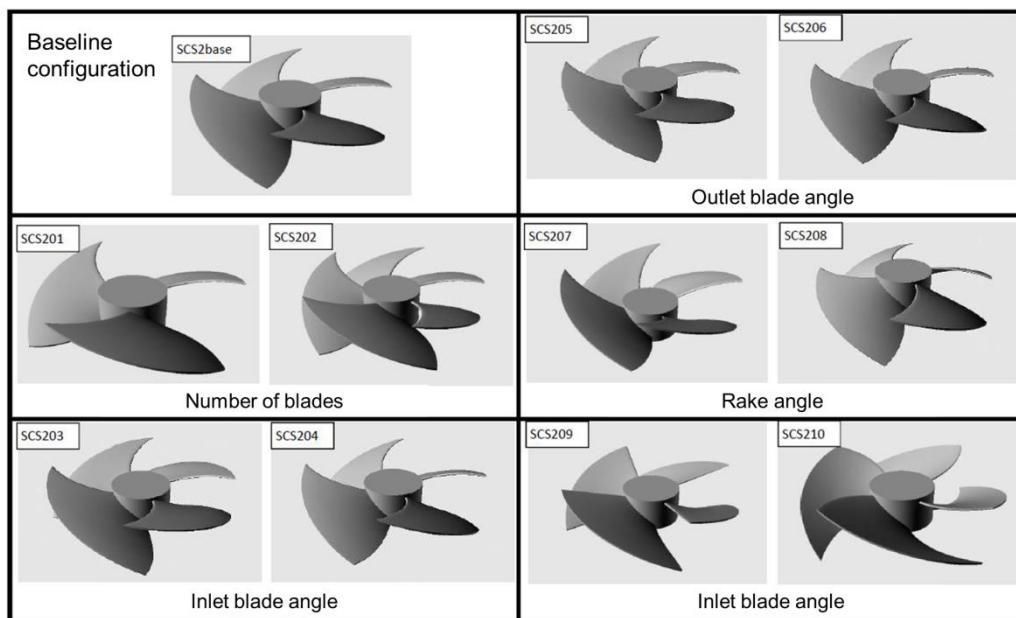
Figure 3: Fan geometrical parameter variations

Experimental setup description

The measurement campaign was conducted in a hemi-anechoic room at Hosei University (Tokyo, Japan). As shown in Figure 4, the fan was mounted on a metal frame at 1.2 m height from the floor without any aerodynamic loading. The fan was attached with a rubber plate which dimension was 120 mm height, 300 mm width and 3 mm thickness, respectively, to avoid any structure borne noise due to the vibrations of the fan.

The rotation speed was forced to 3300 rpm, however, in practice, the actual rotation speed fluctuated by ±15 rpm. The sound pressure level was measured by a class 1 sound level meter, at 1 m in front of the fan, at the same altitude and at 45 degrees on the fan inlet side. The overall background noise level in the anechoic room was around 15 dB, leading to a sufficient signal over noise ratio.
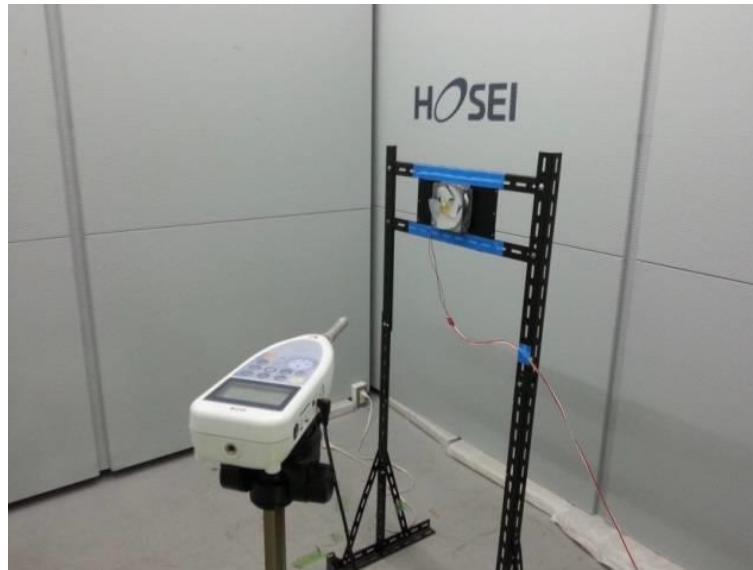
Figure 4: Acoustic measurement of electronic fan in an anechoic chamber

Numerical calculation description

The presented aeroacoustic simulation process is applied on the baseline configuration of the fan (noted SCS2base), as well as on two variants: SCS202 for which 5 blades are considered (instead of 4 blades for SCS2base) and SCS207 where the rake angle of the blades is increased compared to SCS2base. Details on the computation model and run are given on the Baseline case as similar timings and performances are observed on the 2 other configurations.

Figure 5: Description of the studied fan configurations

The CFD model built and run with Cradle scFLOW is presented in Figure 6. It uses a polyhedral mesh of 28 million cells distributed in two regions: a rotating region (~18 M cells) around the fan blades and a static region (~10 M cells) around the rotating region and the fan support. The mesh size in the rotating region is 0.4 mm except in regions where the gap between the blade and the support is very small and the cell size is 0.2 mm. Once the steady simulation is finished, the unsteady simulation starts with a 12.62 µs time step corresponding to 0.25 degrees / cycle. The solution is computed for 6 fan rotations in order to reach convergence. Once this transient solution is over, the flow is considered as in a turbulent regime with converged statistics and the turbulent flow is recorded during 11 additional fan rotations and results are exported every 10 time steps (126 µs). Based on the exported flow solution, the aero-acoustic sources are computed and Fourier transformed up to 4000 Hz to respect the Shanon-Nyquist criterion.

The CFD simulations are performed on a cluster equipped with 28 double Intel E5-2695 v4 nodes (36 core / nodes). The RANS simulation is run over 7 nodes (252 cpus) in 11 hours and 48 minutes and the LES is run over a total of 4 days, 21 hours and 30 minutes.
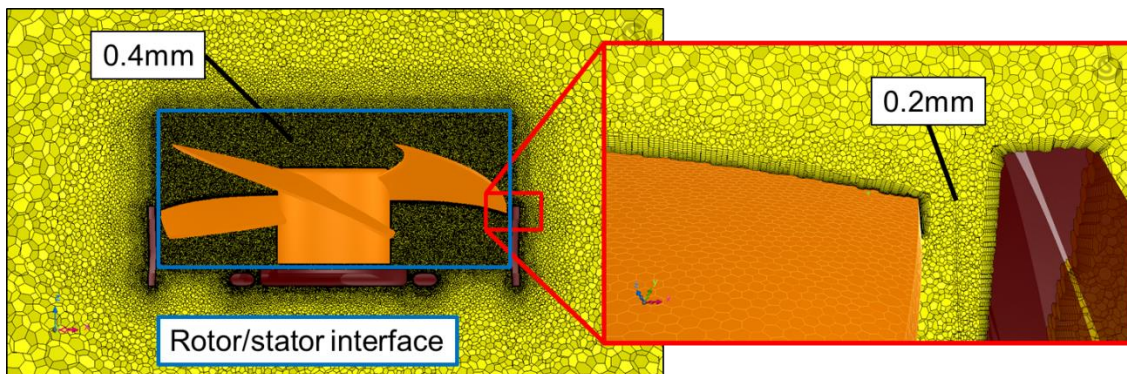

Figure 6: Cut View of the CFD mesh: regions and refinement

The acoustic model generated for the solver FFT Actran is presented in Figure 7. The mesh is generated on the same geometry as the CFD mesh but with specific requirements:

- A surface meshed with triangle elements located at the interface between the stator and rotor regions and used to apply the aero-acoustic excitation.
- A volume mesh with mainly hexahedral elements used to compute the near field propagation of the pressure waves. The volume is meshed using the fan support which will therefore be considered as a rigid wall during the calculation.
- A surface meshed with triangle elements enclosing the volume on which infinite elements are defined. This surface is used to support the infinite elements technology which enforces the non-reflection on this surface and the computation of the results outside the computational domain. Results are exported at the experimental microphone location (1 m in front of the fan, 45° on the side of the fan blowing direction), but the solution is available in the entire domain such that the solution could be recomputed at any virtual microphone after the computation to better understand the acoustic mechanisms.

The acoustic model only covers the static part of the problem so it does not have to be updated in order to run the different blade configurations. All parts of the model are meshed with 7 mm elements designed to support the acoustic radiation at 4000 Hz. This leads to a model with 200·000 degrees of freedom.
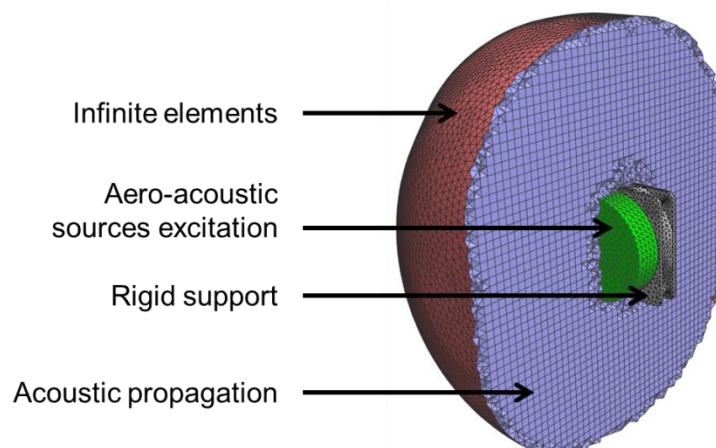

Figure 7: Cut view of the acoustic mesh

The unsteady flow solution is processed to extract and compute the aeroacoustic sources in 12 hours and 30 minutes using four parallel processes requiring 43 GB of RAM each. The aeroacoustic sources are arranged in 8 overlapping samples corresponding to 4 fan rotations. The samples are converted to the frequency domain by a Fourier transform ranging from 13.75 Hz to 3953.15 Hz with a frequency step of 13.75 Hz. The acoustic simulation solves the systems considering the aeroacoustic sources for each frequency in about 2 minutes 30 seconds (on Intel(R) Xeon(R) CPU E3-1240 V2 @ 3.40 GHz). Although the 8 samples are processed at the same time, the solution is classified by samples, and the results are presented by averaging the 8 samples in a similar manner as for experimental results, except that the number of numerical samples is much lower than the number of experimental samples.

Results Presentation and Discussions

The measurements have been performed for several fan designs, leading to an optimized design based on the observations. In this paper, only 3 configurations are tested (baseline and 2 variations) in order to validate the method by comparing the spectrum and the different effects of design changes on the results (Figure 8).
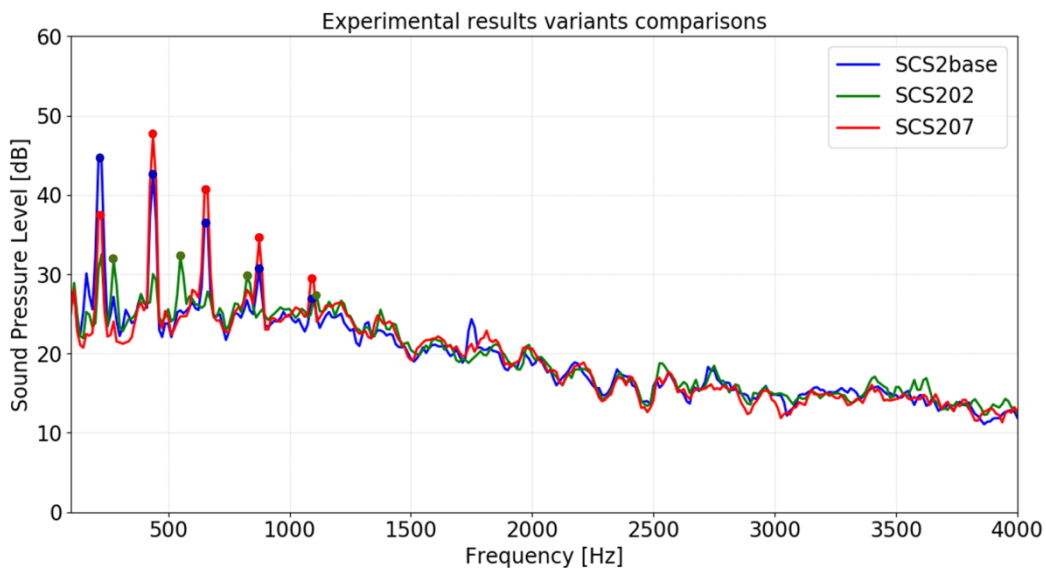

Figure 8: Experimental Sound Pressure Level measurement of three electronic fan parameters variants

The SCS202 configuration has 5 blades whereas the 2 others have 4 blades. This changes the blade passing frequency for the same rotation speed. For the 5 blades fan SCS202, the level of the BPF harmonics only emerges slightly from the broadband noise level. It is also observed that the broadband noise level is very similar for the three variants. The fact that BPF tones are less pronounced for the SCS202 configuration is justified by the two following reasons:

1) As the rotation speed and the back pressure are the same for the 3 configurations, the aerodynamic loading of the 5 blades fan is lower, leading to a reduction of the emergence of the BPF compared to the broadband.
2) As azimuthal mode 5 and harmonics emanating from the 5 blades SCS202 fan have a lower radiation efficiency, the SCS202 fan produce a lower amplitude BPF tones than the two other configurations.

The comparison between measured and simulated sound pressure level for the baseline case is presented in Figure 9.
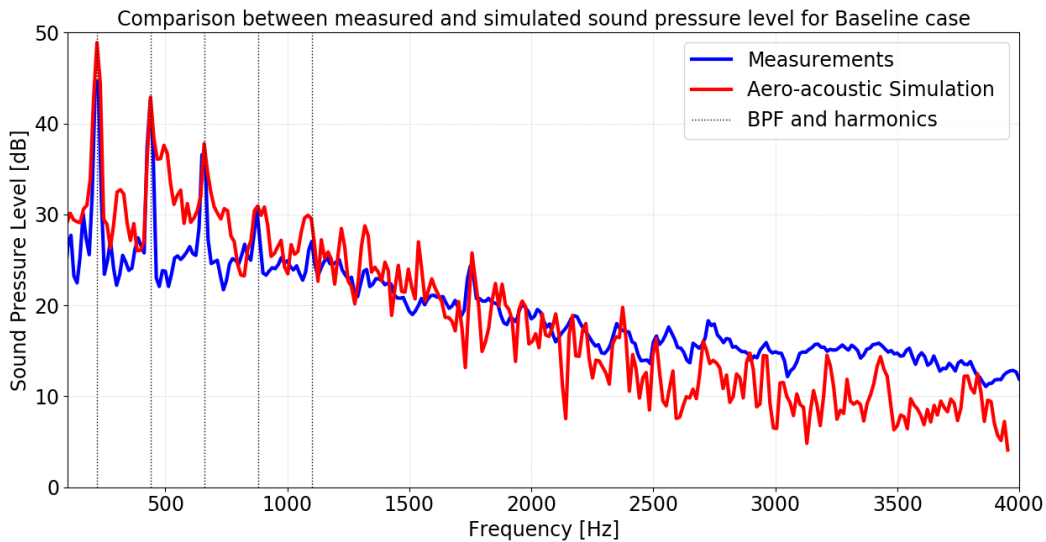
Figure 9: Comparison between measured and simulated sound pressure level for Baseline case (SCS2base)

The noise level at the 4 first BPF harmonics is well captured in the aero-acoustic simulation. The broadband noise tends to be overestimated below 1000 Hz and is then showing a similar trend as the experimental results up to 2000 Hz. At higher frequencies, the predicted sound pressure level is lower than in the experiment.

The overestimation of broadband noise at low frequencies seems to indicate that the level of turbulence downstream the fan blades responsible for the broadband noise is not correctly captured by the flow simulation. These flow inaccuracies may be attributed to various effects including:

1. A lack of convergence of the turbulent flow: e.g. the simulation time may not be sufficient to capture flow recirculating from outlet to inlet as the fan is in an open space,
2. An insufficient number of samples to remove random fluctuations: experimental measurement results are averaged over 550 fan rotations whereas simulation results are averaged over 11 fan rotations,
3. Numerical parameters related to turbulence modeling

The convergence of the numerical results with respect to simulation has been checked over the 11 fan rotations. In Figure 10, the acoustic results are compared for different duration of the numerical used as input for the acoustic simulation. It shows that the acoustic level is relatively stable.
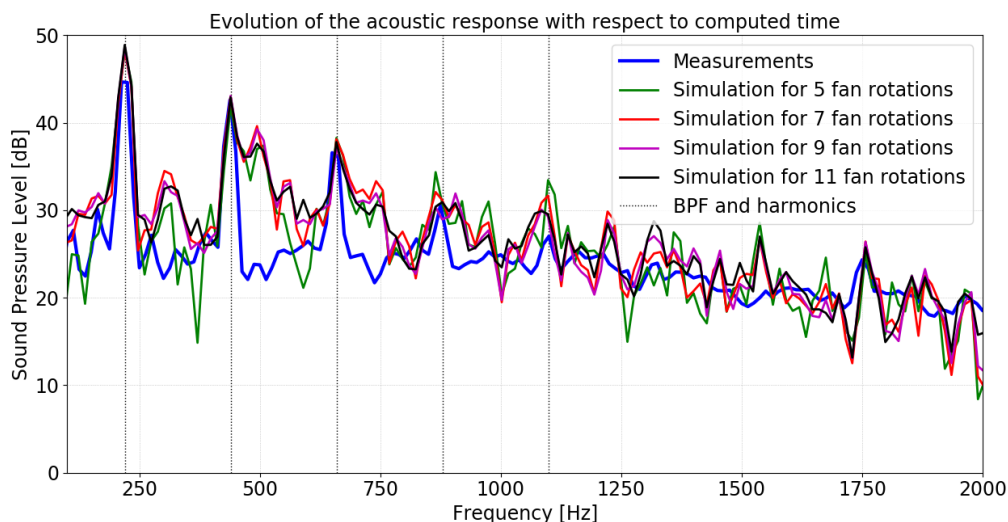

Figure 10: Evolution of sound pressure level with respect to CFD total time

This seems to indicate that the level of turbulence does not decay (or at least slowly) with the simulation duration.

To check if the turbulence level decays during the simulation, longer simulation time would be needed and this has not been investigated in the present paper. Investigations on turbulence modeling parameters are not discussed in the framework of this study.

The difference between numerical and experimental results at higher frequencies is justified by the background level in the experimental facility (15 dB). The high frequency results are therefore measuring partly the background noise level and may not discriminate this from the fan noise. The high frequencies are not affected by aliasing phenomenon providing that the sampling of the turbulent signal satisfies the Shanon-Nyquist theorem. This could be checked by comparing the results with a higher sampling rate than the one selected for the present investigations. This check has not been performed and authors are however confident that no aliasing affects the results presented above.

The comparison between measured and simulated sound pressure level for the SCS202 case (with 5 blades instead of 4) is presented in Figure 11.
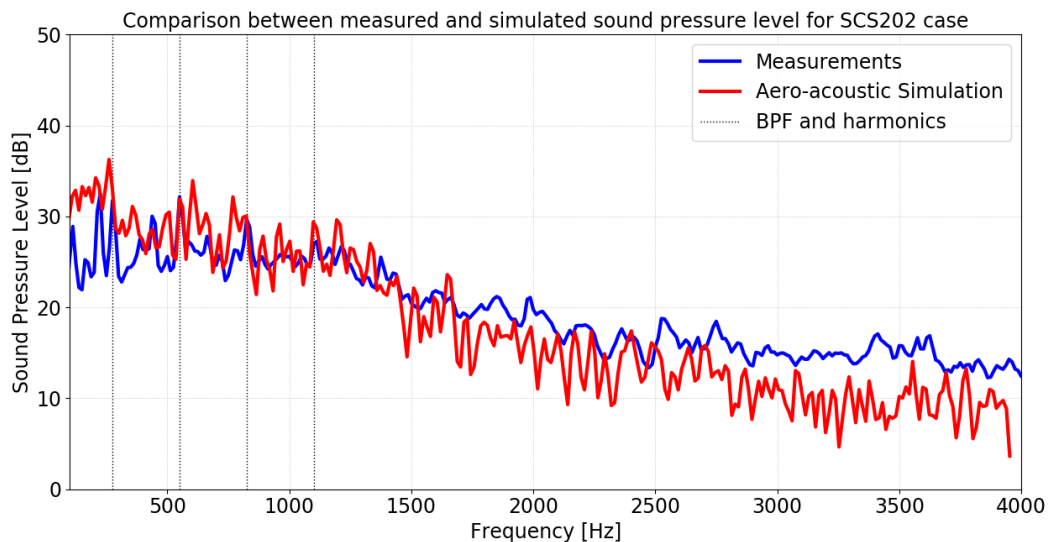

Figure 11: Comparison between measured and simulated sound pressure level for SCS202 case

For the SCS202 configuration, the observations and conclusions derived from baseline configuration are still valid. The level is underestimated above 2000 Hz as the background noise probably affects the measurements. Level at blade passing frequencies is lower than for baseline as confirmed by the experimental results. The broadband noise level differs slightly in the numerical and experimental results as the turbulence level is not perfectly aligned in the numerical flow simulation to the experimental level.

The comparison between measured and simulated sound pressure level for the SCS207 case (with 4 blades and an increased rake angle compared to Baseline) is presented in Figure 12.
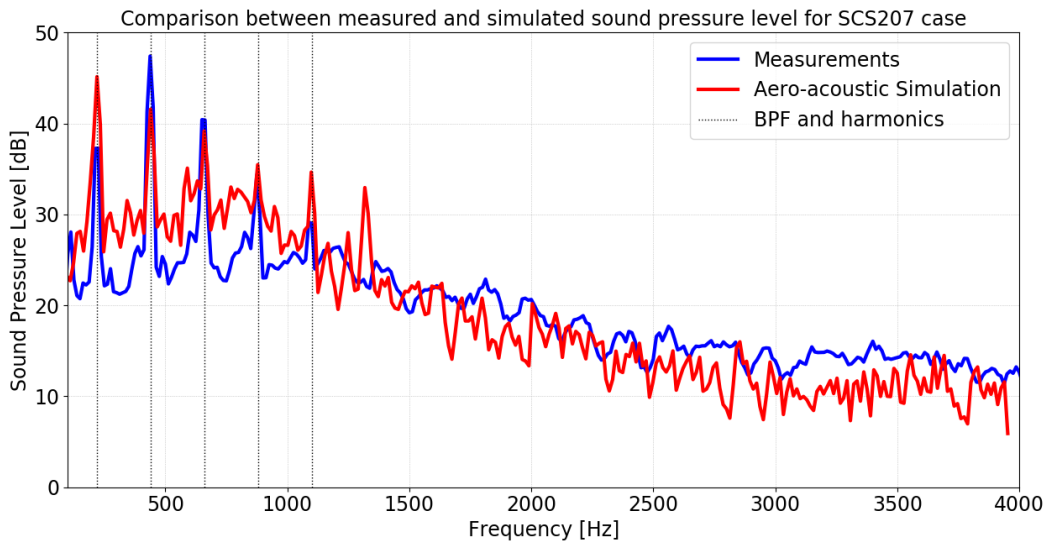
Figure 12: Comparison between measured and simulated sound pressure level for SCS207 case

For this variant, the level of the first BPF harmonic dominates clearly. The level of the first BPF is overestimated, while the second BPF is underestimated in numerical results. Further investigations are ongoing to understand the reasons of these discrepancies. The broadband noise level is over predicted in the numerical results as for the other configurations (background noise level).

CONCLUSIONS

This paper investigates the noise generated by a small axial cooling fan for electronic devices. In general, these fans are integrated to complex channels driving the heat to the outside of the systems and operating with a complex turbulent flow due to heat exchangers or geometrical constraints. Current simulations and experimental investigations have been performed in free field conditions with the fan operating alone in a quiescent medium. Although the noise level is low, this provides a clean and standard condition for comparison and validation of the hybrid method applied in the present paper.

Three different blade designs have been compared to measure the noise improvement with respect to baseline configuration. The different designs correspond to improvements steps in the aerodynamic optimization. These improvements are related to noise reduction at the blade passing frequency and not affecting the broadband noise level.

The simulations are matching to the experimental curves up to the level of background noise present in the experience. The numerical results show the effects of blade design changes on the perceived noise and validate possible integration of this method in an optimization process including the acoustic effects. By visualizing the acoustic pressure and source maps, the method could be used to investigate the noise origin and possibly improve this aspect.

Although the present technique has been applied on clean and quiet operating conditions, it could be used to assess the noise level for real and louder configuration with heat exchanger and turbulent inflow. The noise propagation of this technique is not restricted to free field and can simulate environments including complex acoustic propagation path, acoustic treatments and possibly casing vibrations induced by the flow field.

BIBLIOGRAPHY

[1] F. Menter, "Zonal Two Equation k-ω Turbulence Models for Aerodynamic Flows," *AIAA 93-2906,* 1993.

[2] F. Ducros and F. Nicoud, "Subgrid-scale stress modeling based on the square of the velocity gradient tensor," *Flow turbulence and combustion,* vol. 62, pp. 183-200, 1999.

[3] H. Jasak and e. al., "High resolution NVD differencing scheme for arbitrarily unstructured meshes," *Int. J. Numer. Meth. Fluids,* vol. 31, pp. 431-449, 1999.

[4] M. Lighthill, "On Sound Generated Aerodynamically," *Proc., Roy., Soc., Vol. A211,* 1952.

[5] W. Möhring, "A Well Posed Acoustic Analogy Based on a Moving Acoustic Medium,," in *Proceedings of Aeroacoustics Workshop SWING, edited by P. Költzsch, and N. Kalitzin*, 1999.

[6] M. Cabrol, Y. Detandt, F. Mendonca, D. d'Udekem and J. Manera, "Computational aeroacoustic analysis of industrail fan application using a hybrid approach," in *Fan Noise 2012*, 2012.